Pharm Res (2014) 31:216–227
DOI 10.1007/s11095-013-1154-9

RESEARCH PAPER

In Vivo Fluorescence Imaging of IgG1 Aggregates After Subcutaneous and Intravenous Injection in Mice

Vasco Filipe • Ivo Que • John F. Carpenter • Clemens Löwik • Wim Jiskoot

Received: 17 March 2013 / Accepted: 16 July 2013 / Published online: 15 August 2013

ABSTRACT

Purpose To monitor the biodistribution of IgG1 aggregates upon subcutaneous (SC) and intravenous (IV) administration in mice and measure their propensity to stimulate an early immune response.

Methods A human mAb (IgG1) was fluorescently labeled, aggregated by agitation stress and injected in SKH1 mice through SC and IV routes. The biodistribution of monomeric and aggregated formulations was monitored over 47 days by fluorescence imaging and the early immune response was measured by quantifying the level of relevant cytokines in serum using a Bio-plex assay.

Results The aggregates remained at the SC injection site for a longer time than monomers but after entry into the systemic circulation disappeared faster than monomers. Upon IV administration, both monomers and aggregates spread rapidly throughout the circulation, and a strong accumulation in the liver was observed for both species. Subsequent removal from the circulation was faster for aggregates than monomers. No accumulation in lymph nodes was observed after SC or IV administration. Administration of monomers and aggregates induced similar cytokine levels, but SC injection resulted in higher cytokine levels than IV administration.

Conclusion These results show differences in biodistribution and residence time between IgG1 aggregates and monomers. The long residence time of aggregates at the SC injection site, in conjunction with elevated cytokine levels, may contribute to an enhanced immunogenicity risk of SC injected aggregates compared to that of monomers.

KEY WORDS biodistribution · fluorescence imaging · innate immune response · intravenous · monoclonal antibodies · protein aggregates · subcutaneous

INTRODUCTION

Monoclonal antibodies (mAbs) have proven efficacy in treating a wide range of diseases and have become the dominant fast-growing drug class in the biopharmaceutical industry (1). However, repeated administration of mAbs, as with nearly all other therapeutic proteins, often leads to the induction of antibodies against the protein drug. The presence of anti-drug antibodies may influence pharmacokinetics (PK) and significantly lower the therapeutic efficacy, which in some cases may result in life-threatening consequences (2,3).

Among the several factors playing a role in immunogenicity, the presence of protein aggregates in formulations has been put forward as a major concern (4). It has been shown for different therapeutic proteins that formulations with higher amounts of aggregates tend to be more immunogenic in mouse models (5–9). However, despite this clear direct correlation, the immunological mechanisms behind aggregate-induced immunogenicity remain largely unknown.

Although pharmacokinetic studies are routinely carried out for mAbs, experiments that elucidate underlying mechanisms for biodistribution and clearance of these proteins are not often thoroughly conducted. In fact, there are no reported studies that focus on the biodistribution of aggregates of therapeutic proteins. However, this type of research could

Electronic supplementary material The online version of this article (doi:10.1007/s11095-013-1154-9) contains supplementary material, which is available to authorized users.

V. Filipe · W. Jiskoot (✉)
Division of Drug Delivery Technology
Leiden Academic Center for Drug Research, Leiden University
Einsteinweg 55, 2333 CC Leiden, The Netherlands
e-mail: w.jiskoot@lacdr.leidenuniv.nl

I. Que · C. Löwik
Department of Radiology, Leiden University Medical Centre
Leiden, The Netherlands

J. F. Carpenter
Department of Pharmaceutical Sciences, University of Colorado Denver
Anschutz Medical Campus, Aurora, Colorado 80045, USA

provide valuable information to unveil the starting point of aggregate-related immunogenicity. Differences between the biodistribution of monomers and aggregates may help to explain the reasons why protein aggregates pose an immunological threat.

The biodistribution and clearance of therapeutic proteins depends mainly on the administration route, molecular weight (MW), charge, target and off-target binding properties and immunogenicity (10). Unlike small molecules, which are frequently delivered via oral administration, mAbs are almost exclusively administered by parenteral routes, mainly by intravenous (IV) or subcutaneous (SC) injections. Although most mAbs are delivered IV nowadays, there is a great interest in switching to the SC route to improve patient convenience and potentially reduce treatment costs (11). However, the bioavailability of mAbs following SC administration may vary significantly, ranging from 50% to 100%, and the reasons for such variability are still uncertain (12,13). The mechanisms of mAb absorption from SC tissue are not fully understood, but are influenced by several kinetic processes, including transport through the extracellular matrix, uptake by the blood and lymphatic capillaries and presystemic elimination (14–16).

The high MW of mAbs (150–900 kDa) is above the glomerular filtration cut-off (30–50 kDa), which means that they cannot be eliminated via the kidneys and distribute primarily into vascular space and extracellular fluids (17,18). mAbs are known to be metabolized in several tissues, by circulating phagocytic cells or by their target antigen-containing cells (19). The metabolism of mAbs is relatively slow when compared to other therapeutic proteins, mostly because immunoglobulins are known to be protected from degradation by binding to protective receptors, such as the neonatal Fc-receptor (FcRn), which helps to explain their long elimination half-lives (up to 4 weeks) (20).

Conventional analytical approaches for PK studies of therapeutic proteins rely on enzyme-linked immunosorbent assays (ELISA) of serum or autoradiography with radiolabeled compounds, with ^{125}I being the most commonly used isotope (21,22). ELISA methods are time consuming and labor-intensive and there are several concerns associated with using ^{125}I labeled proteins, such as a rapid loss of ^{125}I label for certain types of molecules and the potential for bioactivity change of biologics during the iodination procedure (22). Meanwhile, new strategies to study the biodistribution of therapeutic proteins are starting to emerge, such as the application of non-invasive fluorescence imaging techniques (23). The technological advances in this area have been remarkable over the last few decades, and the resolution and sensitivity are constantly being improved.

In contrast to the conventional cut-and-count approach or whole-body autoradiography with radiolabeled biologics, fluorescence imaging studies can be conducted in live animals, which provides the advantage of obtaining real-time dynamics on the biodistribution of a therapeutic protein from the same animal. However, it should be pointed out that although fluorescence imaging can provide an overall picture on biodistribution patterns, its sensitivity is still limited compared with autoradiography and therefore the results are only considered qualitative and semi-quantitative (24).

The present work focuses on comparing biodistribution of aggregates and monomers of an IgG1 through the use of live fluorescence imaging techniques. The differences between the biodistribution profiles were analyzed after injection via the two most relevant administration routes for mAbs—SC and IV. The propensity of the monomers or aggregates to induce an early immune response was also evaluated through the measurement of relevant cytokines in blood after injection.

MATERIALS AND METHODS

Protein Formulation

A recombinant human monoclonal antibody of the IgG1 subclass (7) was formulated in 10 mM sodium citrate (Merck, Darmstadt, Germany), 5% (w/v) sucrose (Sigma-Aldrich, Buchs, Switzerland), pH 6.0. The buffer was filtered using a 0.22-μm PES low binding syringe-driven filter unit (Millex™ GP, Millipore, Ireland) prior to any dilution step.

Fluorescent Labeling

IRDye® 800CW and IRDye® RD680 NHS esters were obtained from LI-COR Biosciences (Bad Homburg, Germany). The IgG1 labeling was performed according to the manufacturer's instructions, using a protein concentration of 4 mg/ml and a molar ratio of 3:1 (dye:protein). A pH of 8.0 was chosen for the labeling buffer, in order to achieve selective labeling of the amine termini, but this was not further verified. The labeled IgGs were dialyzed using a 3.5 kDa MWCO Slide-A-Lyzer Cassette (Perbio Science, Etten-Leur, The Netherlands) to remove excess of dye and to exchange from the labeling buffer back to the formulation buffer. The final labeled IgG1 concentration was about 3 mg/ml and the labeling ratio achieved was about 2 labels per IgG1. The labeling ratio was calculated using the absorbance at the excitation maximum of the dyes and protein of the final product, according to the formula provided in the LI-COR protein labeling kit manual. Both 800CW and RD680 labeled IgG1 samples (800CW-IgG1 and RD680-IgG1, respectively) were stored at 4°C.

Aggregate Formation

The IgG1 was stressed in an IKA KS 4000i control shaker (IKA WORKS, Wilmington, NC, USA) by placing 1 ml of

IgG1 solution (0.5 mg/ml) in 2-ml reaction tubes (Eppendorf, Hamburg, Germany) and shaking with orbital agitation at 400 rpm for 3.5 h at room temperature. The tubes were placed horizontally in the shaker to increase the turbulence inside. The samples were stored at 4°C for a maximum period of 24 h until being analyzed or injected.

Size Exclusion Chromatography (SEC)

SEC was performed on a TSK Gel 4000 SWXL column (Tosoh Bioscience, Montgomeryville, PA, USA), using a Thermo Separation Products Spectra System P4000 gradient pump (Thermo Scientific, Breda, The Netherlands), a Waters 717 plus autosampler (Waters, Milford, MA, USA), a Spectra-Physics UV150 UV detector (Spectra-Physics, Irvine, CA, USA) at a 280 nm wavelength and a Waters 2475 fluorescence detector (Waters). For fluorescence detection the samples were excited at 774 nm and the emission spectra were recorded at 789 nm. The data were collected using ADChrom software version 3.5 (Agilent Technologies, Santa Clara, CA, USA). One hundred µl of each sample was injected and separation was performed at a flow rate of 0.5 ml/min. The running buffer was composed of 100 mM sodium phosphate, 100 mM sodium sulfate and 0.05% (w/v) sodium azide at pH 7.1.

Nanoparticle Tracking Analysis (NTA)

NTA measurements were performed with a NanoSight LM20 (NanoSight, Amesbury, United Kingdom), equipped with a sample chamber with a 640-nm laser and a syringe pump. The samples were injected in the sample chamber with sterile BD Discardit II syringes (Becton, Dickinson and Company, Franklin Lakes, NJ, USA) until the liquid reached the tip of the nozzle, and measurements were taken at 27°C with a viscosity of 0.89 cP. The buffer viscosity was measured in an AR-G2 rheometer from TA Instruments (New Castle, DE, USA). The NTA 2.3 software was used for capturing and analyzing the data. The samples were measured at a flow rate of 15 (AU) for 100 s with manual shutter and gain adjustments. Three measurements of each sample were performed and the mean was obtained. The errors reported as shadows in the figures represent the standard deviation between triplicates.

Light Obscuration (LO)

LO measurements were performed on a PAMAS SVSS system (PAMAS GmbH, Rutesheim, Germany) equipped with an HCB-LD-25/25 sensor and a 1-ml syringe. The size range of this analytical tool ranges from 1 µm to 200 µm. Each sample was measured three times, with each measurement consisting of a pre-run volume of 0.3 ml followed by three runs of 0.2 ml at a flow rate of 10 ml/min. The final results are a mean of the three runs and the error bars represent the standard deviation between triplicates. The IgG1 stressed formulation was diluted 5-fold with formulation buffer before the measurement.

Animal Experiment

The mouse strain SKH1 from Charles River Laboratories (Lentilly, France) was chosen for this experiment because it is a hairless and immune-competent strain. A total of 48 female SKH1 mice, age 6 weeks (at the beginning of the experiment), were used in this experiment. The mice were divided in two groups of 24 mice each, one for SC and the other for IV injections. Each of these groups was then divided in subgroups as follows: 8 with 800CW-IgG1 monomers, 8 with 800CW-IgG1 aggregates, 6 with both 800CW-IgG1 aggregates and RD680-IgG1 monomers, 1 with non-reactive free dye as positive control, and 1 without injection as negative control. The total number of control mice was then: 2 negative controls without injection, 1 free dye positive control with SC injection and 1 free dye positive control with IV injection. The groups with both fluorescence dyes were used only for imaging purposes, allowing us to visualize both aggregates and monomers in the same mouse. The groups with only 800CW-IgG1 were used for quantification purposes, i.e. for the quantification of monomeric IgG1 and stressed IgG1 we used the same fluorescent dye that offered the highest sensitivity. From each subgroup, three mice were sacrificed at different time points for organ removal and fluorescence quantification. Blood was collected in Microvette CB 300 heparin tubes (Sarstedt, Germany) at different time points, making a total of three mice per subgroup and per time point.

Each mouse was injected either SC in the dorsal region or IV in the tail vein. The injection volume was: 100 µl of either monomeric or aggregated protein solution (50 µg of protein/injection) for the subgroups administered with only 800CW-IgG1; 100 µl of aggregated 800CW-IgG1 and 100 µl of monomeric RD680-IgG1 protein solution (2 injections of 50 µg of protein/injection) for the subgroups administered with both dyes. All samples were mixed by gently inverting the tubes prior to each injection. This experiment was approved for animal health, ethics, and research by the Animal Welfare Committee of Leiden University Medical Center, The Netherlands (DEC number 12052).

Fluorescence Imaging and Quantification

Images were captured with a Pearl Impulse imager from LI-COR Biosciences (Lincoln, USA) at several time points after injection—1 min, 1 and 5 h and 1, 2, 3, 6, 9, 13, 20, 33 and 47 days. The mice were anesthetized with 2% of isoflurane

and individual images were taken with the mice in dorsal and ventral positions. Some mice were sacrificed during the first time points and whole isolated organs were imaged after removal. The lasers of the Pearl Impulse imager are fixed and optimized for the wavelengths of the two dyes used in this study (685 nm and 785 nm). The images were captured with the Pearl Impulse software v2.0. (LI-COR Biosciences) and two threshold settings were used for making the figures: medium threshold, adjusted to not over expose the initial time point images (Settings 1); and maximum threshold, right below auto-fluorescence in control mice (Settings 2). The regions of interest used for the quantification were chosen according to the type of parameter intended to analyze. Five mice per group were used for the fluorescence quantification of injection site and whole mouse. The error bars represent the standard deviations between the mice.

Cytokines Induction Quantification

Serum cytokine levels were measured with a mouse cytokine 10-Plex panel from Invitrogen (Merelbeke, Belgium) following the manufacturer's instructions. The standards used were the mouse 20-Plex standards from Invitrogen and the formulation buffer was used as a negative control. The samples were analyzed using a Bio-Plex™ Array Reader with Bio-Plex software (Bio-Rad Laboratories, Veenendaal, The Netherlands). The blood samples were stored at −80°C until the day of analysis. Three blood samples per group were used in the assay and the error bars represent the standard deviations between them.

Statistics

Using Graphpad® Prism 5 (GraphPad Software, San Diego CA, USA), a two-way ANOVA test was used to assess statistical difference of fluorescence quantification levels and serum cytokine levels. A calculated probability (P value) equal or below 0.05 was considered to be statistically significant.

RESULTS

Protein Characterization

The level of protein aggregation and free fluorescent dye content were evaluated by SEC with UV and fluorescence detection. NTA and LO were used as complementary techniques to determine the size and number of larger (submicron- and micron-sized) aggregates induced by the stress method. The chromatograms and size distribution graphs of the unstressed and stressed formulation are shown in Fig. 1. The quantification results obtained from these measurements are summarized in Table I. An estimate of the total mass of protein in submicron- and micron-sized aggregates was calculated according to the method described by Barnard *et al.* (25) using the following formula:

$$m_{size\ \ bin} = R \times V \times d \times N$$

with $m_{size\ bin}$ as the estimated protein mass per size bin, R the assumed volume fraction of protein in the particle (=0.75), V the particle volume, d the average protein density (=1.43 g/mL) and N the number of particles per size bin.

The SEC chromatogram of Fig. 1a shows that the agitation method led to approximately 65% monomer loss (eluting at 23 min), but no soluble aggregates could be detected. This indicates that the aggregates formed by this stress method were larger than the interstitial space of the stationary phase and/or contained protein with significantly altered surface properties and therefore could become trapped in the column due to their large size or unspecific interaction with the column material (26). This was confirmed by LO results, in which the number of particles/ml in the micrometer-size range increased 1000-fold after agitation (Fig. 1d). The number of particles in the nanometer-size range, however, remained practically the same after agitation according to NTA results (Fig. 1c). The combination of the results from these three complementary techniques indicates that most of the protein was aggregated after agitation, and that the aggregates were mostly micron-sized. The mass of protein corresponding to the 65% monomer loss (according to SEC) corresponds approximately to the same mass of micron-sized aggregated protein (according to LO) (Table I). The discrepancy between the two protein mass estimations is probably due the different measuring principles, in addition to a certain degree of inaccuracy of the assumption-based method used to calculate the mass of aggregated protein by LO and/or entrapment of (aggregated) protein in the SEC column.

The SEC chromatogram obtained by fluorescence detection shows that the labeling procedure was successful (Fig. 1b). Both unstressed and agitated samples showed monomer peaks eluting at 23 min containing the fluorophore and the ratio between them is similar to that observed by UV detection at 280 nm (cf. Fig. 1a). The fluorescent dye alone eluted at 34 min and none of the protein samples showed a peak at this elution time. This means that the separation between labeled protein and free dye was successful.

In Vivo Fluorescence Imaging

Unstressed RD680-IgG1 and aggregated 800CW-IgG1 were co-administrated SC and IV in mice and fluorescence images were obtained over time. This experimental setting enables the visualization of the biodistribution pattern of both unstressed and stressed IgG1 samples in the same animal. For

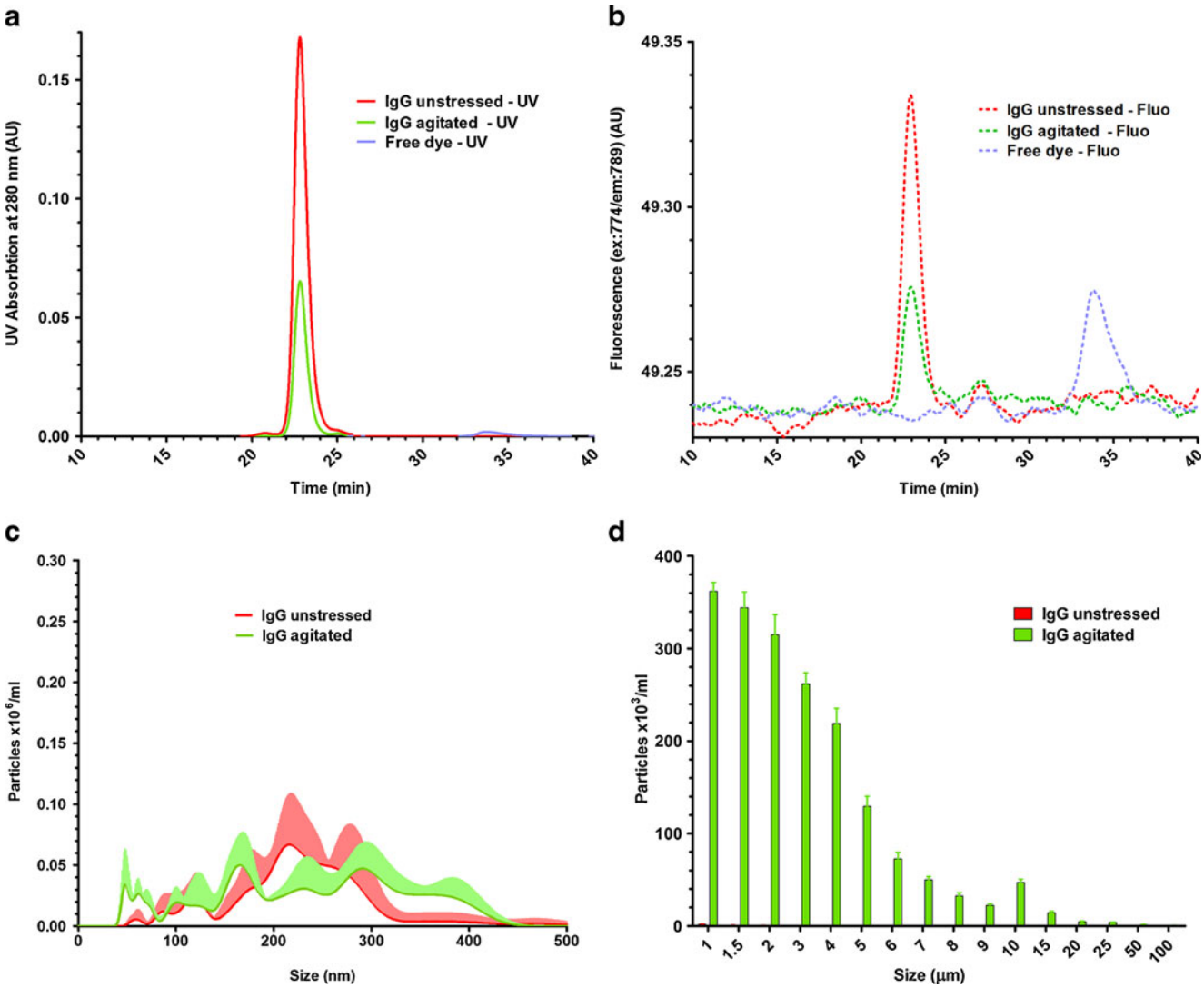

Fig. 1 Aggregation profile of unstressed and agitated 800CW-IgG1 formulations: SEC chromatograms with (**a**) UV detection and (**b**) fluorescence detection; aggregate size distribution measured by (**c**) NTA and (**d**) LO. The NTA and LO graphs contain standard deviations, represented by shadows and error bars, respectively.

SC administration, the injections were given in the dorsal area, whereas IV administration was performed by injecting in the tail vein. The two samples were combined right before IV administration, but injected separately for SC administration. Pilot studies showed no differences between biodistribution patterns of separate or combined SC injections (data not shown). Separate injections were chosen for SC administration because they provide better visualization. The mice were imaged in ventral and dorsal positions for 47 days and the results are shown in Fig. 2 (SC administration) and Fig. 3 (IV administration). The biodistribution trends of the mice not shown in Figs. 2 and 3 were similar to the ones shown in these figures.

Table I Quantification Results from SEC, NTA and LO Analysis. The Mass of Aggregates Corresponds to 100 µl of Sample, i.e. the Injection Volume Used in the Animal Experiments

Sample	SEC		NTA		LO	
	Recovery (%)	Aggregates mass (mg)	Particles × 10^6/ml	Aggregates mass (mg)	Particles × 10^3/ml	Aggregates mass (mg)
Unstressed	100	0	8 ± 2	0.000007 ± 0.000002	4 ± 1	0.00024 ± 0.00004
Agitated	35 ± 5	0.032 ± 0.002	10 ± 2	0.000012 ± 0.000003	1891 ± 104	0.026 ± 0.006

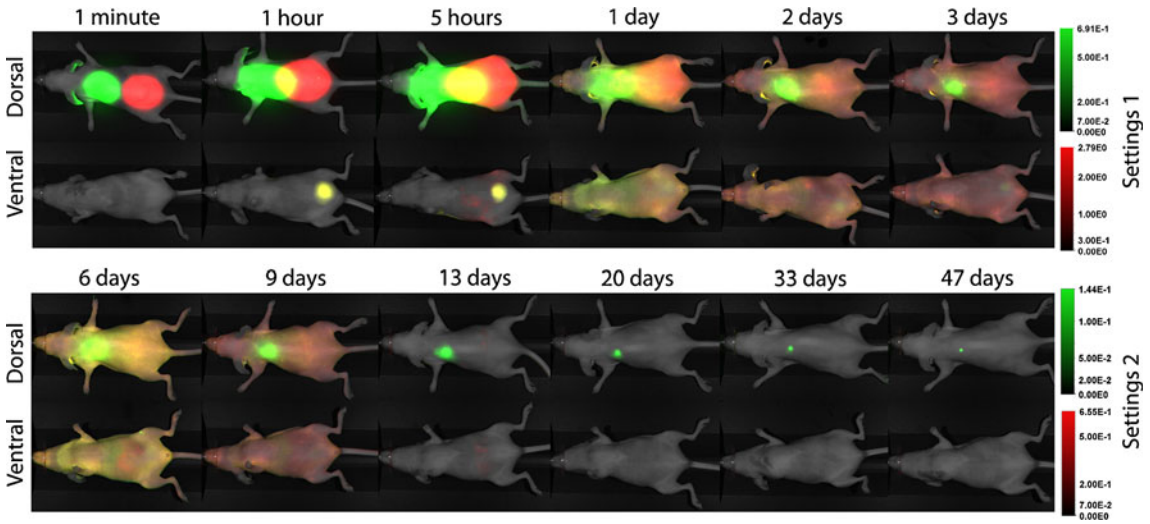

Fig. 2 Representative fluorescence images over time of monomeric RD680-IgG1 (*red*) and aggregated 800CW-IgG1 (*green*) upon SC injections in SKH1 mice. Six mice per group were imaged. Dorsal and ventral images of the same mouse were obtained throughout a time period of 47 days after injection. The aggregates (*green*) were injected in an upper dorsal area, whereas the monomers (*red*) were injected in a lower dorsal area. The overlap of fluorescence signals is displayed as yellow. The fluorescence threshold of the first time points (upper panel) was optimized to not over-expose the first time point (Settings 1). The fluorescence threshold of the last time points (lower panel) was optimized to show the maximum fluorescence possible before auto-fluorescence was reached (Settings 2).

Figure 2 shows that monomers spread faster than aggregated IgG1 from the SC injection site. The difference became clear after 2–3 days, when most of the monomers had already left the injection site, while a considerable amount of aggregates still remained there. The difference became even more obvious at later time points, when aggregates were still visible at the site of injection, even after 47 days.

It took about 24 h for both aggregated and monomeric IgG1 to reach the whole mouse in measurable amounts, presumably through the blood circulation. However, SC spreading may also have contributed to this observation, since the predominant ventral color pattern corresponds to the one observed in the dorsal area. Interestingly, after 3 days the whole ventral area became predominantly red, suggesting that aggregates were removed from circulation faster than monomers. The same tendency was observed at later time points after boosting the fluorescence signals (Settings 2): the ventral area of the mouse changed from yellow (day 6) to red (day 9). The yellow spot in the ventral side at 1 and 5 h corresponds to the bladder, as will be addressed in the "Discussion" section.

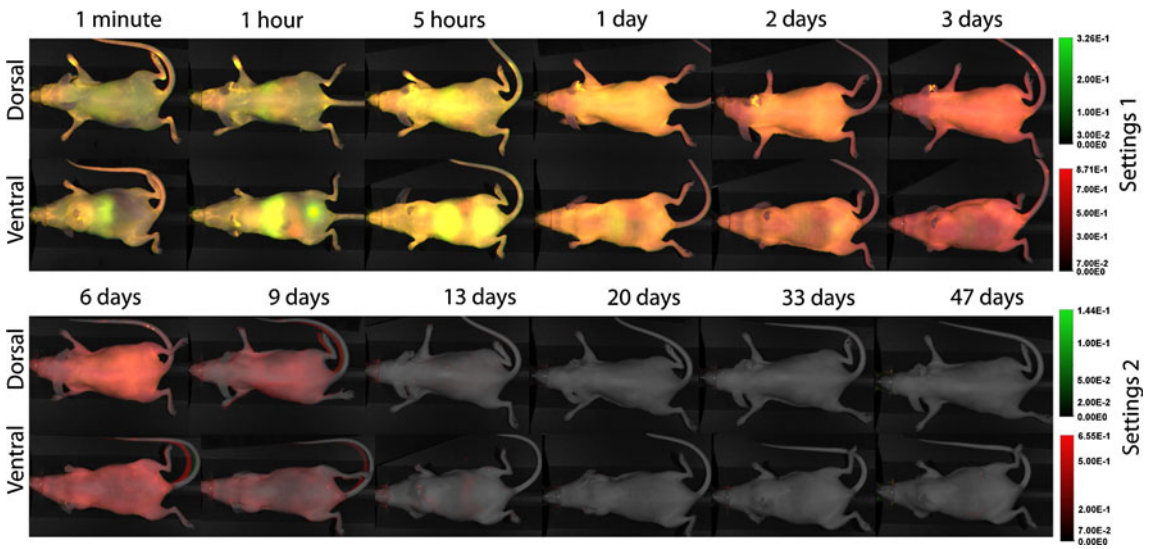

Fig. 3 Representative fluorescence images over time of monomeric RD680-IgG1 (*red*) and aggregated 800CW-IgG1 (*green*) upon IV injection in SKH1 mice. Six mice per group were imaged. Dorsal and ventral images of the same mouse were obtained throughout a time period of 47 days after injection. The two samples were combined right before the injection, which was performed in the tail vein. The overlap of fluorescence signals is displayed as yellow. The fluorescence threshold of the first time points (upper panel) was optimized to not over-expose the first time point (Settings 1). The fluorescence threshold of the last time points (lower panel) was optimized to show the maximum fluorescence possible before auto-fluorescence was reached (Settings 2).

Figure 3 shows that IV injection results in clearly different biodistribution profiles than SC injection, as expected. Both monomers and aggregates spread to the whole body immediately after injection and no accumulation of protein was detected at the injection site. During the first time points (until 5 h), a bright fluorescent spot could be seen in the liver area. The identification of the liver as the organ responsible for this bright spot was made by organ removal of other animals at early time points (Fig. 4). One day after injection this signal considerably faded away.

Similarly to what happened with SC injections, a bright yellow spot was also detected in the bladder area, 1 and 5 h after injection. Likewise, after 3 days the mice became predominantly red, suggesting that also upon IV administration aggregates were removed from circulation faster than monomers. This tendency continued until day 9 and after 13 days the overall fluorescence signal was almost at the level of the negative controls.

Fluorescence Intensity Quantification

Quantification of the fluorescence signals was performed in the groups injected with the same fluorescent dye, i.e. monomeric 800CW-IgG1 and aggregated 800CW-IgG1 groups. The imaging results obtained with the groups injected with the two different dyes were the comparable to the ones injected with the same fluorescent dye (cf. Appendices A and B). The results from the injection site (SC only) and whole mouse (ventral area) are shown in Fig. 5. The quantification results from collected organs are shown in Fig. 4.

The fluorescence signal quantification at the SC injection site (Fig. 5a) confirms that aggregates remain there at significantly higher amounts than monomers ($P=0.0036$). The decay of monomer fluorescence during the first 150 h (~1 week) is remarkably faster than the one of aggregates. It may be important to notice that the plot is in logarithmic scale, to enable the visualization of both the initial and last time points in the same plot. However, contrary to what the images in Fig. 2 suggest, the monomer is not completely out of the injection site after 47 days. According to the quantification results, at this time point the monomer signal is indeed lower than the one of the aggregates, but higher than the control. The difference between the results of Figs. 2 and 5 are probably due to the higher sensitivity of CW800 dye.

The whole-mouse fluorescence quantification results (Fig. 5b) indicate that aggregates disappear from the blood stream significantly faster than monomers, for both administration routes ($P=0.0026$ for IV and $P=0.0022$ for SC). These results are in agreement with the images observed in Figs. 2 and 3. During the first 100 h the fluorescence intensity depends mainly on the

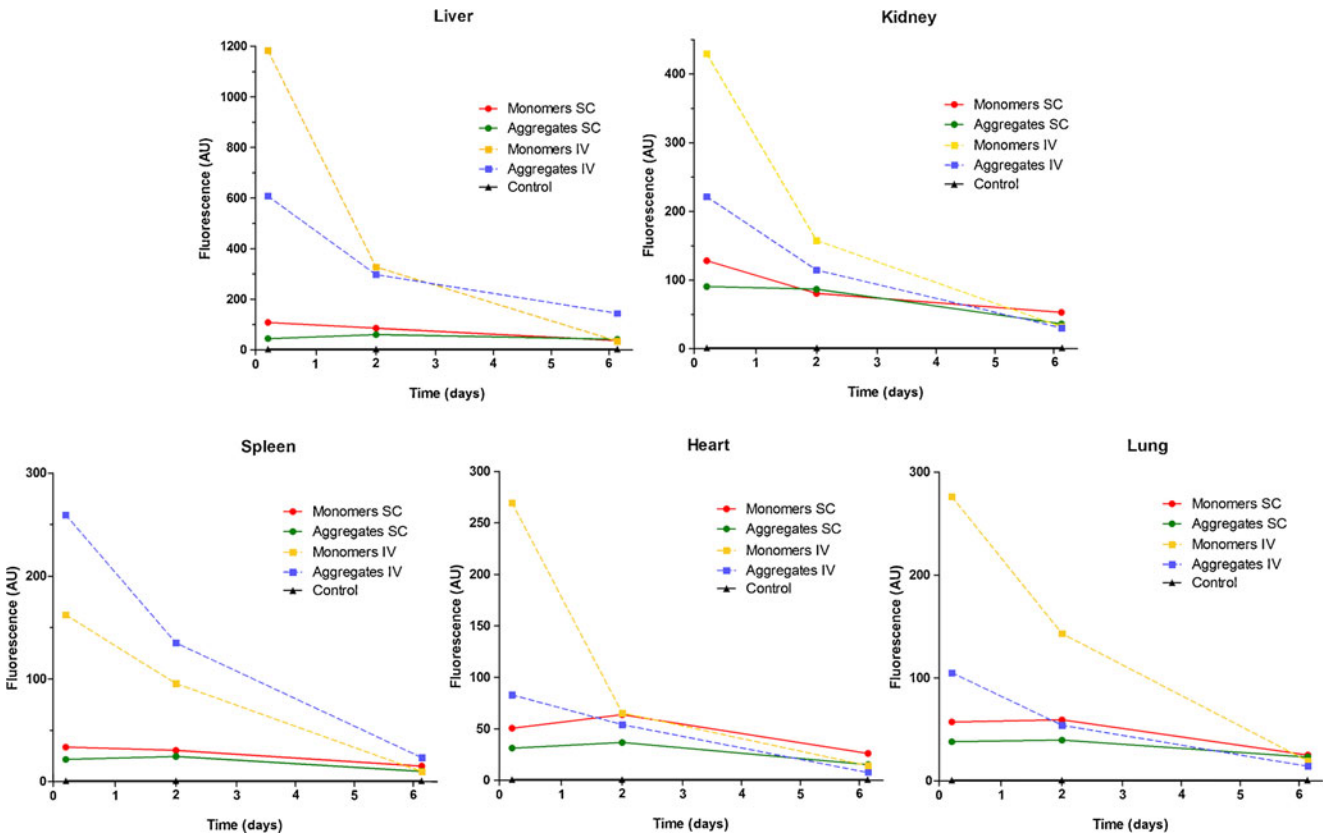

Fig. 4 Fluorescence signal quantification of main organs (*ex vivo*) of monomeric and aggregated 800CW-IgG1 upon SC and IV injection in SKH1 mice. One mouse per time point and per group was used.

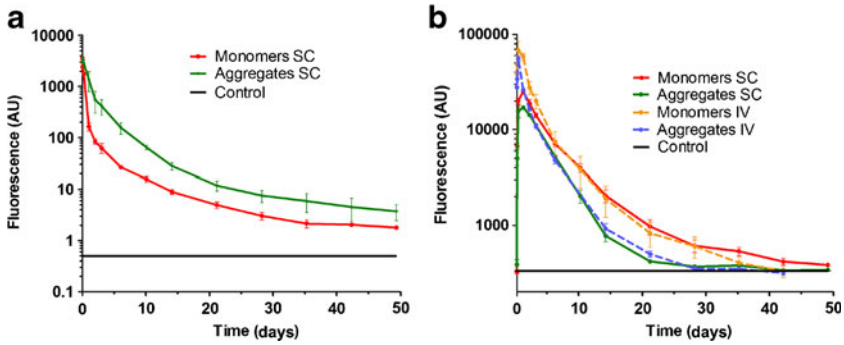

Fig. 5 Fluorescence signal quantification of monomeric and aggregated 800CW-IgG1 upon SC and IV injection in SKH1 mice: (**a**) SC injection site and (**b**) whole-mouse (ventral area). Five mice per group and per time point were used.

injection route and not on the presence of aggregates. The mice administered IV showed extremely high fluorescence immediately after injection, whereas it took a few hours for the maximum level of fluorescence to be reached in mice injected SC. The maximum level of SC injections was about three times lower than the one reached by IV injections. After 200 h, the fluorescence intensity decay depended on the presence of aggregates and not on the administration route anymore. After 1200 h the fluorescence levels of all mice groups was back to the control level. The fluorescence values of the whole mouse quantification cannot be directly compared to the ones of the injection site since different regions of interest were used.

Some mice were sacrificed during the first time points and their main organs were removed and their fluorescence was quantified (Fig. 4). Only one mouse per time point was analyzed and therefore no statistical significance can be taken from these results. Nevertheless, it is clear that both monomeric and aggregated IgG1 strongly accumulated in the liver upon IV administration, confirming the whole mouse imaging results (cf. Fig. 3). The organ with the second highest fluorescence upon IV administration was the kidney. The heart, spleen and lung showed similar levels of fluorescence after IV injections: between the respective controls and the kidney levels. The spleen was the only organ that showed higher levels for aggregates than for monomers. SC administration increased the fluorescence values almost equally in all the organs, but less than in the organs after IV administration.

Cytokine Induction Quantification

The propensity of SC and IV administered IgG1 monomers and aggregates to trigger an early immune response was measured by quantifying the concentration of 10 cytokines in blood samples collected during the first week after injection: interleukin (IL)-1β, IL-2, IL-4, IL-5, IL-6, IL-10, IL-12, granulocyte-macrophage colony-stimulating factor (GM-CSF), interferon-gamma (IFN-γ and tumor necrosis factor-alpha (TNF-α. All these cytokines are involved in inflammatory pathways and their up-regulation is normally associated with increased

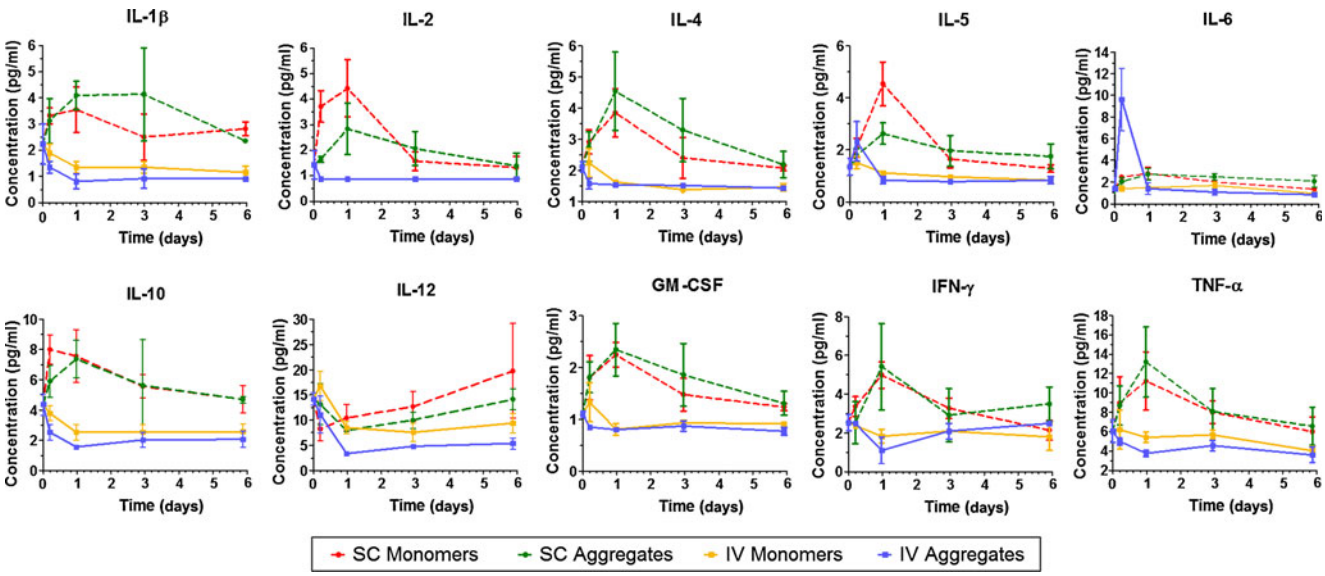

Fig. 6 Bio-plex analysis of inflammatory cytokines in serum of SKH1 mice administered with either monomeric or aggregated 800CW-IgG1, injected either SC or IV. Serum from three mice per group and per time point was used.

immune response activity (27). Their blood levels were measured by Bio-plex analysis and the results are shown in Fig. 6.

The serum concentration of all cytokines was very low and close to the lower detection limit of the technique. Nevertheless, significant differences were observed between overall cytokine levels of mice injected through different administration routes: SC injections induced higher overall cytokine levels than IV injections ($P=0.0278$). However, no differences were observed between monomers and aggregates ($P=0.5009$). The only cytokine that showed a distinctly higher concentration with aggregates than monomers after IV administration was IL-6, but only at one time point (5 h).

DISCUSSION

The formation of aggregates is inherent to the manufacturing and storage of therapeutic proteins. Even though there is a generalized concern about the presence of protein aggregates in therapeutic formulations, very little is known about their fate upon administration. In this work the biodistribution patterns of IgG1 aggregates following SC and IV injection, in comparison with those of IgG1 monomers, were analyzed and their propensity to stimulate an early immune system was evaluated.

A human IgG1 was chosen for this study because it represents the majority of mAbs in development and clinical phases nowadays (28). One of the main concerns regarding biodistribution studies of human proteins in animals is their foreign nature. Foreign proteins normally induce immune responses, which may affect the biodistribution profiles. However, previous studies with this particular human IgG1 have shown that aggregate-free formulations are not immunogenic in mice, even after repeated administration (7).

Another major issue that can affect the biodistribution of human mAbs in mice is their affinity to the murine FcRn receptor. The role of FcRn in modifying the systemic half-life of mAbs is well known (20,29). It has been shown that this receptor plays also a major role in SC absorption of mAbs (14,30,31). Since the binding affinity of human IgG1 to murine FcRn receptor has shown to be very high according to Andersen *et al.* (32), we expect that the results obtained in this study are representative for what may happen in humans.

The method chosen to induce aggregation was agitation stress, mainly because it creates a high percentage of mainly small micron-sized aggregates. Little is known about the influence of aggregate size on immunogenicity, but small micron-sized aggregates have been receiving a lot of attention from pharmaceutical companies and regulatory agencies because of their potential immunogenicity in conjunction with the fact that they have been analytically overlooked until recent years (33). The agitation method used in this study induced approximately 65% aggregation according to SEC results. The ideal sample would have been 100% aggregated, but that turned out to be very difficult to achieve. Any attempt to increase the percentage of aggregates resulted in considerable protein precipitation (data not shown).

Fluorescence imaging results show that IgG1 aggregates disappeared faster than monomers from circulation. This is in good agreement with the studies performed by Gamble, in which he observed an inversed correlation between the amount of aggregates and the serum half-life of iodine I-131 Ig in mice (5). The most likely explanations for this occurrence are: physical blockage of aggregates in certain organs/tissues due to their high MW; aggregates cannot bind to the FcRn receptor; or aggregates are captured and degraded by macrophages (e.g., in the spleen) and other immune cells (34).

Small micron-sized particles in circulation have been shown to accumulate mainly in the liver and spleen (35). In this study, aggregates did seem to accumulate more in the spleen than monomers, but the only organ that showed significant accumulation of 800CW-IgG1 was the liver (after IV administration). Quantification results in the liver (Fig. 4) show that for monomeric IgG1 the level of fluorescence is higher than that for stressed IgG1 during the first time points. This suggests that physical blockage of aggregates is probably not the predominant mechanism for the accumulation observed in this organ. However, the liver contains specialized macrophages—Kupffer cells—known for efficiently binding and phagocytosis of aggregated IgG1 via specific Fc receptors (36,37). Thus, it is possible that the lower fluorescence observed for the aggregates in liver was the immediate result of their degradation by Kupffer cells.

The strong fluorescence signal observed in the bladder during the first time points of Fig. 2 and 3 is most likely caused by free dye, given that IgGs are too large to undergo glomerular filtration. This assumption was confirmed by injecting unreactive free dye in control animals. These showed the same bladder fluorescence during the first hours after injection, but not the liver fluorescence (Appendix C). Moreover, a fluorescence lifetime imaging study showed that the fluorescence lifetime in the bladder was similar to that of free IRDye® 800CW (ca. 0.55 ns), whereas the fluorescence lifetime of labeled 800CW-IgG1 was about 0.80 ns, similar to the average fluorescence lifetime over the whole body of mice injected with 800CW-IgG1 (unpublished data). All the free dye was cleared after 24 h for both injection routes. The presence of free dye in labeled mAb formulations was quite surprising since SEC results show no free dye at all (Fig. 1). One possible explanation for this is that dye molecules could have been (non-covalently) bound to the mAb. This noncovalent association could have been strong enough to resist SEC mobile phase conditions, similar to what has been observed for noncovalent fluorescent dyes (38), but not strong enough to survive under *in vivo* conditions. The covalent peptide bond between the IgG1 and the fluorescent label is very stable and it

is not expected to break during the first few hours after injection. Nevertheless, it is possible that a percentage of the fluorescence detected in the bladder a few hours after injection is the consequence of some degree of label-bond instability or the formation of small label-containing IgG1 fragments.

The cytokine signature used in the study carried by Joubert *et al.* served as a base for our choice of cytokines. They showed that mechanically stressed IgG with a high amount of aggregates (2–10 μm) significantly enhance the *in vitro* innate immune response of a population of naïve human peripheral blood mononuclear cells (27). Four of the cytokines present in the signature associated with mechanically induced aggregates were tested (IL-1β, IL-6, IL-10, and TNF-α), as well as six other cytokines involved in innate and/or adaptive immune responses (IL2, IL4, IL5, IL12, GM-CSF and IFNγ). Since the experimental setting consisted of a single injection, the cytokine levels were measured only during the first 6 days after injection. The mice injected with aggregates showed the same levels of inflammatory cytokines as the ones injected with monomers. It is important to notice that cytokine concentrations detected in serum are lower than the ones obtained in cell culture *in vitro*, mostly due to their short half-life and because they can be taken up taken up by neighboring cells. The cytokine serum concentrations obtained in this study were almost at the lower detection limit of the analytical technique and that may account for the lack of detected differences between aggregates and monomers. Nevertheless, the assay was sensitive enough to detect significant differences between the two injection routes. The SC route induced a higher cytokine response than the IV route. This, together with our observation that aggregates remain very long at the SC injection site, might explain why in general it is thought that SC administration has a higher immunogenicity risk than IV administration (33,39–41), although there are exceptions to this rule (42).

Following SC administration, therapeutic proteins have been shown to pass through regional lymph nodes before they reach the systemic circulation (43,44). A positive correlation has been shown between a protein's MW and the percentage of the dose that is taken up by the lymphatic system in sheep (45). In the present work, no lymph node accumulation was detected for either aggregates or monomers (cf. Fig. 2). These results are not consistent with the findings of Wu *et al.*, in which they observed the accumulation of RD680-bevacizumab in axillary lymph nodes of SKH1 mice upon front pad SC injection (46). However, other studies have shown that the anatomic site of injection has a major impact on both the rate and extent of absorption, which is reflected in the lymph node accumulation (47,48). It is thus possible that the conditions used in our study were not sensitive enough to detect the accumulation of labeled protein in draining lymph nodes. Nevertheless, our observation is in agreement with the findings of Kagan *et al.*, who concluded that the lymphatic system contributes minimally to the overall bioavailability of SC administered proteins in rats (14,31,47).

It should be noted that the formulation used in this study deliberately contained a significantly higher amount of aggregates compared to aggregate levels typically found in commercial therapeutic products. Therefore, these results may not be representative of what happens during the clinical use of therapeutic proteins. Nevertheless, the current experimental settings were appropriate to show differences in biodistribution profiles between monomers and aggregates.

CONCLUSIONS

In this study we aimed to identify any differences in biodistribution and immune response profiles between IgG1 aggregates and monomers that could eventually correlate with aggregate-induced immunogenicity. A human IgG1 was fluorescently labeled, aggregated by agitation stress and injected in mice through SC and IV routes. The biodistribution and early immune response of monomers and aggregates were compared. The aggregates remained at the SC injection site for a longer time but disappeared from the systemic circulation faster than monomers did (for both SC and IV routes). A strong accumulation in the liver was observed for both monomeric and aggregated species upon IV administration. No lymphatic node accumulation was observed for SC administrations. Surprisingly, no differences were observed in cytokine levels between mice injected with monomers and aggregates. However, there was a remarkable difference between the two injection routes: SC administration induced higher overall cytokine levels than the IV route. This, in conjunction with the long residence time of aggregated protein at the SC injection site, may contribute to an increased immunogenicity risk of therapeutic proteins when administered SC relative to IV administration.

ACKNOWLEDGMENTS AND DISCLOSURES

The authors acknowledge Els van Beelen for her help with the Bio-Plex assay.

REFERENCES

1. Lawrence S. Pipelines turn to biotech. Nat Biotechnol. 2007;25:1342.
2. Chirmule N, Jawa V, Meibohm B. Immunogenicity to therapeutic proteins: impact on PK/PD and efficacy. AAPS J. 2012;14:296–302.
3. Schellekens H. Immunogenicity of therapeutic proteins: clinical implications and future prospects. Clin Ther. 2002;24:1720–40. discussion 1719.
4. Rosenberg AS. Effects of protein aggregates: an immunologic perspective. AAPS J. 2006;8:E501–507.

5. Gamble CN. The role of soluble aggregates in the primary immune response of mice to human gamma globulin. Int Arch allergy Appl immunol. 1966;30:446–55.
6. Braun A, Kwee L, Labow MA, Alsenz J. Protein aggregates seem to play a key role among the parameters influencing the antigenicity of interferon alpha (IFN-alpha) in normal and transgenic mice. Pharm Res. 1997;14:1472–8.
7. Filipe V, Jiskoot W, Basmeleh AH, Halim A, Schellekens H. Immunogenicity of different stressed IgG monoclonal antibody formulations in immune tolerant transgenic mice. MAbs. 2012;4:740–75.
8. van Beers MM, Sauerborn M, Gilli F, Brinks V, Schellekens H, Jiskoot W. Oxidized and aggregated recombinant human interferon beta is immunogenic in human interferon beta transgenic mice. Pharm Res. 2011;28:2393–402.
9. Hermeling S, Schellekens H, Maas C, Gebbink MF, Crommelin DJ, Jiskoot W. Antibody response to aggregated human interferon alpha2b in wild-type and transgenic immune tolerant mice depends on type and level of aggregation. J Pharm Sci. 2006;95:1084–96.
10. Ferraiolo BL, Mohler MA, Gloff CA. Protein pharmacokinetics and metabolism. New York: Plenum Press; 1992.
11. Bittner B, Richter WF, Hourcade-Potelleret F, McIntyre C, Herting F, Zepeda ML, *et al.* Development of a subcutaneous formulation for trastuzumab—nonclinical and clinical bridging approach to the approved intravenous dosing regimen. Arzneimittelforschung. 2012;62:401–9.
12. Lobo ED, Hansen RJ, Balthasar JP. Antibody pharmacokinetics and pharmacodynamics. J Pharm Sci. 2004;93:2645–68.
13. Dirks NL, Meibohm B. Population pharmacokinetics of therapeutic monoclonal antibodies. Clin Pharmacokinet. 2010;49:633–59.
14. Kagan L, Gershkovich P, Mendelman A, Amsili S, Ezov N, Hoffman A. The role of the lymphatic system in subcutaneous absorption of macromolecules in the rat model. Eur J Pharm Biopharm. 2007;67:759–65.
15. Wang W, Chen N, Shen X, Cunningham P, Fauty S, Michel K, *et al.* Lymphatic transport and catabolism of therapeutic proteins after subcutaneous administration to rats and dogs. Drug Metab Dispos. 2012;40:952–62.
16. Porter CJ, Charman SA. Lymphatic transport of proteins after subcutaneous administration. J Pharm Sci. 2000;89:297–310.
17. Baumann A. Early development of therapeutic biologics–pharmacokinetics. Curr Drug Metab. 2006;7:15–21.
18. Tang L, Persky AM, Hochhaus G, Meibohm B. Pharmacokinetic aspects of biotechnology products. J Pharm Sci. 2004;93:2184–204.
19. Keizer RJ, Huitema AD, Schellens JH, Beijnen JH. Clinical pharmacokinetics of therapeutic monoclonal antibodies. Clin Pharmacokinet. 2010;49:493–507.
20. Kuo TT, Aveson VG. Neonatal Fc receptor and IgG-based therapeutics. MAbs. 2011;3:422–30.
21. DeSilva B, Smith W, Weiner R, Kelley M, Smolec J, Lee B, *et al.* Recommendations for the bioanalytical method validation of ligand-binding assays to support pharmacokinetic assessments of macromolecules. Pharm Res. 2003;20:1885–900.
22. Vugmeyster Y, DeFranco D, Szklut P, Wang Q, Xu X. Biodistribution of [125I]-labeled therapeutic proteins: application in protein drug development beyond oncology. J Pharm Sci. 2010;99:1028–45.
23. Leblond F, Davis SC, Valdes PA, Pogue BW. Pre-clinical whole-body fluorescence imaging: Review of instruments, methods and applications. J Photochem Photobiol B. 2010;98:77–94.
24. Hillman EM, Amoozegar CB, Wang T, McCaslin AF, Bouchard MB, Mansfield J, *et al.* In vivo optical imaging and dynamic contrast methods for biomedical research. Philos Transact A Math Phys Eng Sci. 2011;369:4620–43.
25. Barnard JG, Singh S, Randolph TW, Carpenter JF. Subvisible particle counting provides a sensitive method of detecting and quantifying aggregation of monoclonal antibody caused by freeze-thawing: insights into the roles of particles in the protein aggregation pathway. J Pharm Sci. 2011;100:492–503.
26. Philo JS. A critical review of methods for size characterization of non-particulate protein aggregates. Curr Pharm Biotechnol. 2009;10:359–72.
27. Joubert MK, Hokom M, Eakin C, Zhou L, Deshpande M, Baker MP, *et al.* Highly aggregated antibody therapeutics can enhance the in vitro innate and late-stage T-cell immune responses. J Biol Chem. 2012;287:25266–79.
28. Nelson AL, Dhimolea E, Reichert JM. Development trends for human monoclonal antibody therapeutics. Nat Rev Drug Discov. 2010;9:767–74.
29. Oganesyan V, Damschroder MM, Woods RM, Cook KE, Wu H, Dall'acqua WF. Structural characterization of a human Fc fragment engineered for extended serum half-life. Mol Immunol. 2009;46:1750–5.
30. Wang W, Wang EQ, Balthasar JP. Monoclonal antibody pharmacokinetics and pharmacodynamics. Clin Pharmacol Ther. 2008;84:548–58.
31. Kagan L, Mager DE. Mechanisms of subcutaneous absorption of rituximab in rats. Drug Metab Dispos. 2013;41:248–55.
32. Andersen JT, Daba MB, Berntzen G, Michaelsen TE, Sandlie I. Cross-species binding analyses of mouse and human neonatal Fc receptor show dramatic differences in immunoglobulin G and albumin binding. J Biol Chem. 2010;285:4826–36.
33. Carpenter JF, Randolph TW, Jiskoot W, Crommelin DJ, Middaugh CR, Winter G, *et al.* Overlooking subvisible particles in therapeutic protein products: gaps that may compromise product quality. J Pharm Sci. 2009;98:1201–5.
34. Robinson WL. Some points of the mechanism of filtration by the spleen. Am J Pathol. 1928;4:309–20. 303.
35. Tasciotti E, Godin B, Martinez JO, Chiappini C, Bhavane R, Liu X, *et al.* Near-infrared imaging method for the in vivo assessment of the biodistribution of nanoporous silicon particles. Mol Imaging. 2011;10:56–68.
36. Bogers WM, Stad RK, Janssen DJ, van Rooijen N, van Es LA, Daha MR. Kupffer cell depletion in vivo results in preferential elimination of IgG aggregates and immune complexes via specific Fc receptors on rat liver endothelial cells. Clin Exp Immunol. 1991;86:328–33.
37. Helmy KY, Katschke Jr KJ, Gorgani NN, Kljavin NM, Elliott JM, Diehl L, *et al.* CRIg: a macrophage complement receptor required for phagocytosis of circulating pathogens. Cell. 2006;124:915–27.
38. Hawe A, Friess W, Sutter M, Jiskoot W. Online fluorescent dye detection method for the characterization of immunoglobulin G aggregation by size exclusion chromatography and asymmetrical flow field flow fractionation. Anal Biochem. 2008;378:115–22.
39. Singh SK, Afonina N, Awwad M, Bechtold-Peters K, Blue JT, Chou D, *et al.* An industry perspective on the monitoring of subvisible particles as a quality attribute for protein therapeutics. J Pharm Sci. 2010;99:3302–21.
40. Ismael G, Hegg R, Muehlbauer S, Heinzmann D, Lum B, Kim SB, *et al.* Subcutaneous versus intravenous administration of (neo)adjuvant trastuzumab in patients with HER2-positive, clinical stage I-III breast cancer (HannaH study): a phase 3, open-label, multicentre, randomised trial. Lancet Oncol. 2012;13:869–78.
41. Hermeling S, Crommelin DJ, Schellekens H, Jiskoot W. Structure-immunogenicity relationships of therapeutic proteins. Pharm Res. 2004;21:897–903.
42. Kijanka G, Jiskoot W, Schellekens H, Brinks V. Effect of treatment regimen on the immunogenicity of human interferon beta in immune tolerant mice. Pharm Res. 2013;30:1553–60.
43. McLennan DN, Porter CJ, Edwards GA, Heatherington AC, Martin SW, Charman SA. The absorption of darbepoetin alfa occurs predominantly via the lymphatics following subcutaneous administration to sheep. Pharm Res. 2006;23:2060–6.
44. Charman SA, McLennan DN, Edwards GA, Porter CJ. Lymphatic absorption is a significant contributor to the subcutaneous bioavailability of insulin in a sheep model. Pharm Res. 2001;18:1620–6.

45. McLennan DN, Porter CJ, Edwards GA, Martin SW, Heatherington AC, Charman SA. Lymphatic absorption is the primary contributor to the systemic availability of epoetin Alfa following subcutaneous administration to sheep. J Pharmacol Exp Ther. 2005;313:345–51.
46. Wu F, Bhansali SG, Law WC, Bergey EJ, Prasad PN, Morris ME. Fluorescence imaging of the lymph node uptake of proteins in mice after subcutaneous injection: molecular weight dependence. Pharm Res. 2012;29:1843–53.
47. Kagan L, Turner MR, Balu-Iyer SV, Mager DE. Subcutaneous absorption of monoclonal antibodies: role of dose, site of injection, and injection volume on rituximab pharmacokinetics in rats. Pharm Res. 2012;29:490–9.
48. Kota J, Machavaram KK, McLennan DN, Edwards GA, Porter CJ, Charman SA. Lymphatic absorption of subcutaneously administered proteins: influence of different injection sites on the absorption of darbepoetin alfa using a sheep model. Drug Metabol Dis Biol Fate Chem. 2007;35:2211–7.